Design of Fractional-Order PID Controller for Trajectory Tracking Control of Continuum Robots

Ayman Belkhiri
Assistant Professor
Department of Mechanical Engineering,
Laboratory of Mechanics, Frères Mentouri
Constantine 1 University
Algeria

Ammar Amouri
Associate Professor, HDR
Department of Mechanical Engineering,
Laboratory of Mechanics, Frères Mentouri
Constantine 1 University
Algeria

Abdelhakim Cherfia
Associate Professor, HDR
Department of Mechanical Engineering,
Laboratory of Mechanics, Frères Mentouri
Constantine 1 University
Algeria

Continuum robots are the behavioral extension of hyper-redundant robots usually inspired by living biological organs. These robots outperform their rigid counterparts regarding high flexibility, dexterity, and most importantly safe interaction. On the flip side, they are kinematically redundant, highly nonlinear, and multi-input, and consequently, their controlling remains a complex and challenging task. To this end, this paper proposes a Fractional-Order Proportional-Integral-Derivative (FOPID) controller to control the continuum robot's end-tip. The proposed controller is designed to control the inputs of a class of continuum robots, namely the Cable-Driven Continuum Robot (CDCR). To design the controller satisfactorily, the Particle Swarm Optimization (PSO) algorithm extracts the optimal values of the controller's parameters. The proposed FOPID controller's efficiency and control performance are demonstrated through two simulation examples: set-point tracking and point-to-point trajectory tracking. In addition, the obtained simulation results are compared to those provided by classical and Optimized PID controllers and to some available schemes. Given the obtained results, it is clear that the performances of the proposed FOPID controller are superior in tracking accuracy and smoothness in control signals.

Keywords: *Continuum robot, cable-driven continuum robot, fractional-order PID controller, particle swarm optimization, trajectory tracking.*

1. INTRODUCTION

Recently, continuum robots have been given great importance in healthcare, rescue missions, and many other industrial applications. Due to their lightweight and high flexibility, they can perceive, operate, and maneuver easily in confined spaces and complex environments where rigid-link robots cannot operate [1-2]. In literature, many classes of continuum robots have been developed, fabricated, and commercialized, including soft continuum robots [3], fluid-driven continuum robots [4], tendon-driven continuum robots [5], bellows-driven continuum robots [6], and cable-driven Continuum robots (CDCR) [7]. In the same context, other kinds of robots are developed based on experience inspired by nature [8-9]. However, developing effective controllers is still an ongoing need due to the complexity of their mathematical models and the resulting modeling inaccuracies.

Although continuum robotic structures introduce significant complexity in modeling, significant progress has been made in continuum robots, including kinematics and dynamics. Among the contributions to the kinematics modeling of continuum robots, one can cite the works presented in [10-13]. In these works, different methods and theories have been used. Most of them are based on the so-called Constant Curvature Kinematic Approach [14], which is a reduced kinematic model commonly used in continuum robotics due to its simplicity. Accordingly, many research works have been carried out to study the dynamic behavior of different types of continuum robots. Regarding the continuum robots class considered here, namely Cable-Driven Continuum Robot (CDCR), different principles and methods have been used to establish their dynamics models, such as the principle of virtual power [15-16], Euler-Lagrange method [17-20], and Newton-Euler method [21-22]. Among these kinematic and dynamic models used as a general framework for control pur–poses, one can cite the works presented in [12-13, 17].

Admittedly, controlling continuum robots has so far been a laborious duty. Despite that, great efforts are being made to apply classical and advanced control techniques to address the control problem. Focusing on CDCR's control, only some works have been proposed. A Nonlinear Model Predictive Control (NMPC) is proposed to solve the trajectory tracking and obstacle avoidance problems for planar and spatial CDCR using kinematic and dynamic models [13, 23]. In [24], the authors applied a nonlinear sliding mode control-based-adaptive particle swarm optimization algorithm to control the CDCR's end-tip in the planar case. Other researchers have used classical PID controllers to ensure trajectory tracking [17].

Although the above works significantly contribute to controlling CDCRs, these control schemes have some limitations, especially when considering the tracking accuracy and real-time implementation, controlling CDCRs is still in its infancy and remains a challenging task. In a first attempt to bridge this gap, the present

Received: September 2022, Accepted: April 2023
Correspondence to: Dr. Ayman Belkhiri
Department of Mechanical Engineering, Frères Mentouri Constantine 1 University, Algeria.
E-mail: ayman.belkhiri@umc.edu.dz
doi: 10.5937/fme2302243B

paper aims to harness the advantages of fractional calculus by designing and implementing a Fractional-Order Proportional-Integral-Derivative (FOPID) controller for the sake of controlling a Cable-Driven Continuum Robot (CDCR). Indeed, the FOPID controller tends to perform better than the classical PID version due to characteristics like the nonlinear nature and the two extra tuning parameters that allow more flexibility and a better adjustment in the controller action. However, FOPID's parameter tuning is a difficult task. To this end, the Particle Swarm Optimization (PSO) algorithm has been used to achieve this purpose such as in [25-26]. In this context, one can cite, for example, the recent contributions to FOPID robotics control, including mobile robots [27-28], serial robot manipulators [29-30], parallel robots [31], as well as for rigid mechanisms such as the scissor mechanism platform [26].

To do so, the subsequent Sections of the paper are structured as follows: the next Section describes the mathematical models, including both kinematic and dynamic models, of the considered CDCR with two sections. Section 3 focuses on FOPID controller development and the tuning process of the controller's parameters based on the Particle Swarm Optimization (PSO) algorithm. Simulation results for set-point tracking and point-to-point trajectory tracking, illustrating the effectiveness and performance of the proposed controller are presented in Section 4. Concluding remarks and perspectives of this work are given in Section 5.

2. MATHEMATICAL MODELS OF THE CDCR

Based on the Constant Curvature Kinematic Approach (CCKA) [14], this Section summarizes the kinematics and dynamic models of the CDCR under consideration. The scheme design of the CDCR under consideration is illustrated in Figure 1. It is one of the most popular continuum robots, with three actuators per Section.

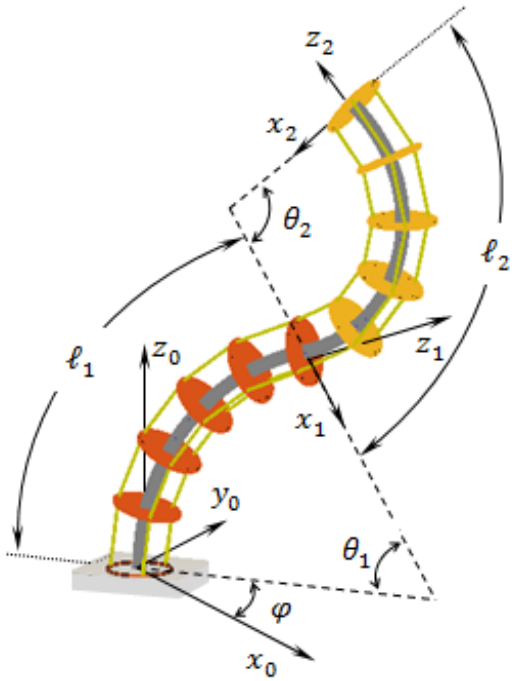

Figure 1. CDCR schematics

Pursuing control and trajectory tracking objectives, hereafter, we present and exploit the mathematical equations governing the kinematics and dynamics of the considered CDCR [17].

2.1 Kinematics models

This subsection provides the kinematics of the CDCR, including local and global coordinates, rotation matrices, and linear and angular velocities. A set of generalized coordinates and velocities are needed to describe the dynamic configuration of the CDCR under consideration. Therefore, the position vector Pk, with k = 1,2 of each CDCR's section end-tip with respect to the robot's reference base and the associated rotation matrix R_k can be calculated recursively as follows:

$$\mathrm{P}_k = \begin{cases} \mathrm{P}_{1,lcl}, & k=1 \\ \mathrm{P}_{1,lcl} + \mathrm{R}_{1,lcl}\mathrm{P}_{2,lcl}, & k=2 \end{cases} \tag{1}$$

$$\mathrm{R}_k = \begin{cases} \mathrm{R}_{1,lcl}, & k=1 \\ \mathrm{R}_{1,lcl}\mathrm{R}_{2,lcl}, & k=2 \end{cases} \tag{2}$$

such as the local position vector $\mathrm{P}_{k,lcl}$ and the local rotation matrix $\mathrm{R}_{k,lcl}$ of each CDCR's Section with respect to its reference base are given as follows:

$$\mathrm{P}_{k,lcl} = \begin{cases} x_k = \rho\ell_k\left(\dfrac{\theta_k}{2} - \dfrac{\theta_k^3}{24}\right), \\ y_k = \sigma\ell_k\left(\dfrac{\theta_k}{2} - \dfrac{\theta_k^3}{24}\right), \\ z_k = \ell_k\left(1 - \dfrac{\theta_k^2}{6} + \dfrac{\theta_k^4}{120}\right), \end{cases} \tag{3}$$

$$\mathrm{R}_{k,lcl} = \begin{bmatrix} \rho & -\sigma & 0 \\ \sigma & \rho & 0 \\ 0 & 0 & 1 \end{bmatrix} \begin{bmatrix} C_{\theta_k} & 0 & -S_{\theta_k} \\ 0 & 1 & 0 \\ S_{\theta_k} & 0 & C_{\theta_k} \end{bmatrix} \begin{bmatrix} \rho & \sigma & 0 \\ -\sigma & \rho & 0 \\ 0 & 0 & 1 \end{bmatrix}, \tag{4}$$

where $\rho = C_{\theta_k}$ is a constant and $\sigma = \sqrt{1-\rho^2}$. $C_{(\cdot)}$ and $S_{(\cdot)}$ are the cosine and the sine functions, respectively.

For further use, the local rotation matrix $\mathrm{R}_{k,lcl}$ is written as a function of unit vectors, as follows:

$$\mathrm{R}_{k,lcl} = \begin{bmatrix} \mathrm{n}_{k,lcl} & \mathrm{b}_{k,lcl} & \mathrm{t}_{k,lcl} \end{bmatrix}, \tag{5}$$

where $\mathrm{n}_{k,lcl}$, $\mathrm{b}_{k,lcl}$ and $\mathrm{t}_{k,lcl}$ are the normal vector, the binormal vector, and the tangent vector, respectively.

By deriving Eq. 1 with respect to time, the linear velocity of each CDCR's section end-tip in the robot's reference base can be expressed as follows:

$$\mathrm{P}_k = \begin{cases} \dot{\mathrm{P}}_{1,lcl}, & k=1 \\ \dot{\mathrm{P}}_{1,lcl} + \dot{\mathrm{R}}_{1,lcl}\mathrm{P}_{2,lcl} + \mathrm{R}_{1,lcl}\dot{\mathrm{P}}_{2,lcl}, & k=2 \end{cases} \tag{6}$$

Moreover, for simplicity reasons, the angular velocity ω_k is calculated as a function of the tangent vector, as follows:

$$\omega_k = \begin{cases} \omega_{1,lcl}, & k=1 \\ \omega_{1,lcl} + \mathrm{R}_{1,lcl}\omega_{2,lcl}, & k=2 \end{cases} \quad (7)$$

such as the local angular velocity $\omega_{1,lcl}$ is given as follows:

$$\omega_{k,lcl} = \mathrm{t}_{k,lcl} \times \dot{\mathrm{t}}_{k,lcl}, \quad (8)$$

where $\dot{\mathrm{t}}_{k,lcl}$ is the derivative vector with respect to the time of the third column of the rotation matrix $\mathrm{R}_{k,lcl}$, and "$\times$" refers to the cross product.

2.2 Dynamic model

In this paper, the dynamic model is a cornerstone element of the control law design strategy. Therefore, by using the Euler-Lagrange method for the generalized coordinates θ_k, with $k=1, 2$, the dynamic model of the considered CDCR can be represented by a system of two coupled nonlinear differential equations, as follows:

$$\begin{bmatrix} \mathrm{M}_{11} & \mathrm{M}_{11} \\ \mathrm{M}_{11} & \mathrm{M}_{11} \end{bmatrix} \begin{Bmatrix} \ddot{\theta}_1 \\ \ddot{\theta}_2 \end{Bmatrix} + \begin{bmatrix} \mathrm{M}_{11} & \mathrm{M}_{11} & \mathrm{M}_{11} \\ \mathrm{M}_{11} & \mathrm{M}_{11} & \mathrm{M}_{11} \end{bmatrix} \begin{Bmatrix} \dot{\theta}_1^2 \\ \dot{\theta}_1\dot{\theta}_2 \\ \dot{\theta}_2^2 \end{Bmatrix} + \begin{Bmatrix} \mathrm{K}_1 \\ \mathrm{K}_1 \end{Bmatrix} = \begin{Bmatrix} \mathrm{Q}_1 \\ \mathrm{Q}_1 \end{Bmatrix} \quad (9)$$

The dynamical model should be represented in the state space to simulate and analyze the input-output behavior of the considered CDCR. Thus, by introducing the state variables, Eq. 9 can be written in the general form as follows:

$$\dot{\mathrm{s}}(t) = \mathrm{f}(\mathrm{s},t) + \mathrm{h}(\mathrm{s},t) \cdot \mathrm{u}(t) \quad (10)$$

where s(t) is the state variables vector given by Eq. 11. f(s,t) and h(s,t) are nonlinear functions. u(t) is the command vector, and is the time parameter.

$$\mathrm{s}(t) = \begin{cases} \mathrm{s}_1 = \theta_1(t), \\ \mathrm{s}_2 = \dot{\theta}_1(t), \\ \mathrm{s}_3 = \theta_2(t), \\ \mathrm{s}_4 = \dot{\theta}_2(t), \end{cases} \quad (11)$$

3. FRACTIONAL ORDER CONTROLLER DESIGN

3.1 Fractional order control

The generalization of the classical integer calculus, subsequently called fractional calculus, was first mentioned in a letter between Leibniz and L'Hospital over three centuries ago [32]. However, the idea remained a purely mathematical matter for a long time. Many researchers have recently focused on fractional calculus topics, and great efforts have been made to discover its applications in science and engineering. In the field of control systems, for instance, the earliest attempt was made by I. Podlubny in 1999, who introduced the Fractional-Order Proportional-Integral-Derivative controller [33]. The new controller can be abbreviated with FOPID and symbolized as $\mathrm{PI}^{\lambda}\mathrm{D}^{\mu}$ controller. It is a generalization of the classical PID controller, which results in higher flexibility and capability due to its two additional parameters, namely: the fractional order of the integral λ and the derivative μ whose their values can be given with any arbitrary real number where their values are chosen generally within the range from 0 to 2. Figure 2 summarizes the relationship between the classical PID and FOPID controllers as a function of the two parameters λ and μ. For instance, when the values of both parameters (λ,μ) are equal to 1, the FOPID and PID controller is the same. The common categories of PID controllers, namely: Proportional (P), Proportional-Integral (PI), and Proportional-Derivative (PD) controllers, are obtained when the values of both parameters (λ,μ) equal to (0, 0), (1, 0), and (0, 1), respectively (see, Figure 2). The governing equation of the FOPID controller in the time domain can be expressed as follows:

$$\mathrm{u}(t) = K_{\mathrm{P}}\, e(t) + K_{\mathrm{I}}\, D^{-\lambda}\, e(t) + K_{\mathrm{D}} D^{\mu}\, e(t), \quad (12)$$

where K_{p}, K_{I}, and K_{D} denote the proportional, integral and derivative coefficients, respectively. λ and μ are the integral and derivative order, respectively. u(t) and (t) are the input and output in the time domain of the controller, respectively. $D^{(\cdot)}$is a generalized operator of integration and differentiation, a mix process commonly applied in fractional calculus topics (for more details, we refer the reader to references [34-35]).

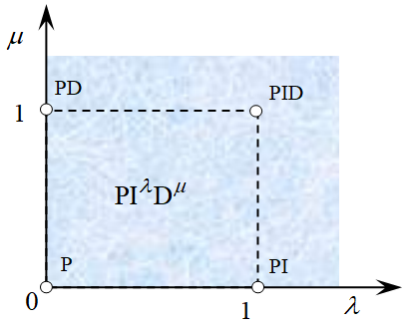

Figure 2. Relationships between PID's categories and FOPID controllers

It is worth noting that the FOPID controller gives additional specifications and improves the robustness of the controlled system, however, parameters tuning is a difficult task because most robotic systems, including the considered CDCR, are often featured by a complex behavior. For such reasons, a particle swarm optimi–zation (PSO) algorithm is introduced here to tune the parameters of the proposed controller.

3.2 PSO algorithm

Nowadays, meta-heuristic algorithms are widely used to optimize high-complexity problems in various sciences and engineering fields [36-39]. Hereby, thanks to its simplicity, the particle swarm optimization (PSO) algo–rithm [40] is adopted to extract the optimal parameters of the proposed controller, thanks to its simplicity [41]. In PSO algorithm, a set of particles moves in the search space looking for the optimal values of a performance

index called cost function. At each iteration *iter*, each particle *p* changes its velocity and position as a function of its local best position P_{pbest}^{iter} and the global best position P_{gbest}^{iter} according to the following equations:

$$\mathrm{v}_p^{iter+1} = w\mathrm{v}_p^{iter} + \mathrm{r}_1\mathrm{c}_1\left(P_{pbest}^{iter} - \mathrm{x}_p^{iter}\right) + \mathrm{r}_2\mathrm{c}_2\left(P_{gbest}^{iter} - \mathrm{x}_p^{iter}\right), \tag{13}$$

$$\mathrm{x}_p^{iter+1} = \mathrm{x}_p^{iter} + \mathrm{v}_p^{iter+1}, \tag{14}$$

where w is the inertia weight rate; v_p^{iter} is the current velocity of particle pth at iteration *iter*; x_p^{iter} is the current position of particle pth at iteration *iter*; r_1 and r_2 are two random variables between 0 and 1; c_1 and c_2 are cognitive and social coefficients, respectively.

Although the PSO algorithm has many advantages, including simple implementation and its fast conver–gence ability with few tuned parameters [42-43], the convergence towards an optimal solution is not guaranteed. However, to avoid the early convergence towards the local minima, the regenerating of popu–lation technique has been added to the PSO algorithm [41, 44]. The block diagram of a PSO algorithm is given in Figure 3.

3.3 FOPID controller structure

To control the position of the considered CDCR's end-tip, two discrete FOPID controllers are implemented. One controller is designed to control the bending angle of the first Section, and the other controls the second Section's bending angle. However, because the two sections of the robot share the same geometrical and inertial characteristics and properties, the five para–meters of the two controllers are chosen to be similar. The schematic diagram of the proposed controller is shown in Figure 4, and the control laws $\mathrm{u}_1(t)$ and $\mathrm{u}_2(t)$ are given as follows:

$$\begin{cases} \mathrm{u}_1(t) = K_\mathrm{P}\, e_1(t) + K_\mathrm{I}\, D^{-\lambda}\, e_1(t) + K_\mathrm{D} D^{\mu}\, e_1(t), \\ \mathrm{u}_2(t) = K_\mathrm{P}\, e_2(t) + K_\mathrm{I}\, D^{-\lambda}\, e_2(t) + K_\mathrm{D} D^{\mu}\, e_2(t), \end{cases} \tag{15}$$

where $\mathrm{e}_1(t)$ and $\mathrm{e}_2(t)$ represent the tracking errors between the desired and generated bending angles θ_1 and θ_2, respectively.

In fact, to obtain satisfactory control performance, the three coefficients K_P, K_I, K_D and the two non-integer parameters (λ,μ) should be optimally determined. To achieve this purpose, the tuning of these parameters, as a closed loop system such that the robot satisfies the desired specifications, is described below.

3.4 Tuning PI$^{\lambda}$D$^{\mu}$ of parameters

This part aims to extract the optimal values of the FOPID controller's parameters using the Particle Swarm Optimization (PSO) algorithm. In practice, the main step in applying the PSO algorithm is to choose the best cost function used to evaluate each particle's fitness. Thus, the appropriate cost function to be minimized can be defined simply by the performance index given by the square error of the two outputs, as follows:

$$C_f = \sqrt{e_1^2(t) + e_2^2(t)} \tag{16}$$

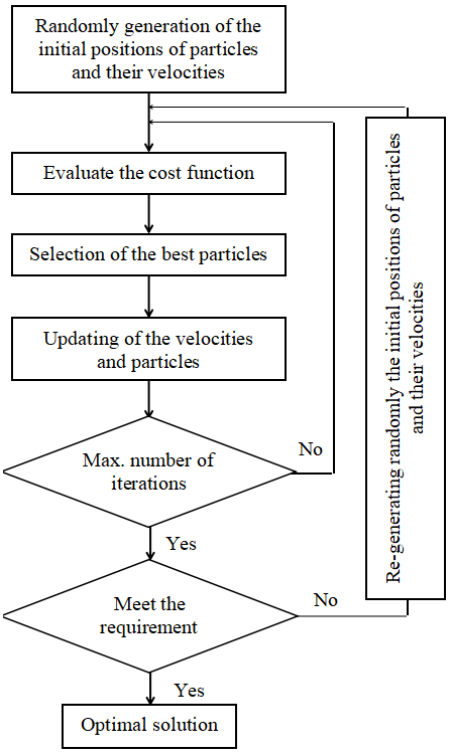

Figure 3. Block diagram of PSO algorithm

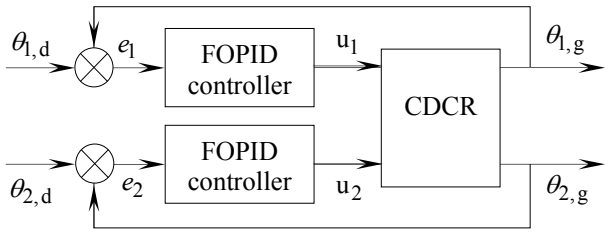

Figure 4. Schematic diagram of the proposed FOPID controllers

In the search space, the dimension of the optimization problem is (1×5). The population in PSO is the set of possible solutions, and the particles are the variables of the optimization problem, which represent here the five FOPID controller's parameters, namely: the three coeffi–cients K_p, K_I, K_D and the two non-integer parameters (λ,μ). The tuning process of the FOPID cont–roller's parameters with PSO algorithm is shown in Figure 5.

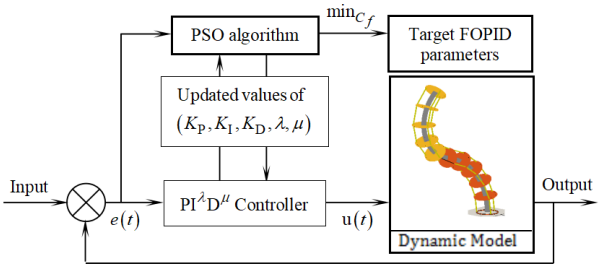

Figure 5. FOPID controller's parameters tuning using PSO algorithm

4. SIMULATION AND ANALYSIS

Two simulation examples are carried out to verify the proposed controller's performance and effectiveness. The first simulation focuses on set-point tracking, while the second is devoted to tracking a circular trajectory. Besides, to highlight the control performance, a comparative study for both simulation examples was conducted between the proposed controller and the two PID controller categories: classical PID controller and OPID controller. Simulations are carried out in a MATLAB environment. The main parameters used for the robotic system simulation are listed in Table 1 [17], and the optimal controller parameters are given in Table 2. For both simulation examples, the sampling time is chosen as 0.005 sec.

4.1 Set-point tracking

To evaluate the performance of the proposed FOPID controller, $\theta_{1,d} = 2\theta_{2,d} = \pi/3$ as set-point tracking is chosen for both sections of the considered CDCR. Figure 6 highlights the tracking performance of the proposed controller compared to the classical and optimized PID ones in which the Mean Squared Error (MSE) and the Mean Absolute Error (MAE) are computed for each one (see Table 3). According to the results, the proposed controller gives better control performance than others. Specifically, the averages of MSE and MAE of the proposed controller are lower than those of the OPID controller; see gray boxes in Table 3.

Table 1. Geometric and material of the simulated CDCR

Par.	Designation	Value
l_k	Section length	0.3 m
m	Disk mass	0.01 kg
E	Young's modulus	210 GPa
I_d	Inertia moment of disk	$3.97 \cdot 10^{-12}$ m^4
I_{xx}	Backbone inertia	$3.06 \cdot 10^{-7}$ m^4

Table 2. Optimal parameters of the considered controllers

	FOPID	OPID	PID	PID [17]
K_P	1.1863	1.0964	1.1863	0.1
K_I	4.2258	5.7056	4.2258	2.7
K_D	3.01705	0.7885	3.01705	0.3
λ	0.998	1	1	1
μ	0.768	1	1	1

Table 3. Recorded MSE and MAE values in case of set-point tracking for both sections

Controllers	MSE		MAE	
	θ_1	θ_2	θ_1	θ_2
FOPID	0.0519	0.0072*	0.0841	0.0325*
OPID	0.0494*	0.0110	0.0785*	0.0402
PID	0.0524	0.0089	0.0847	0.0326
PID [17]	0.0945	0.0231	0.1704	0.0850
*Best value				

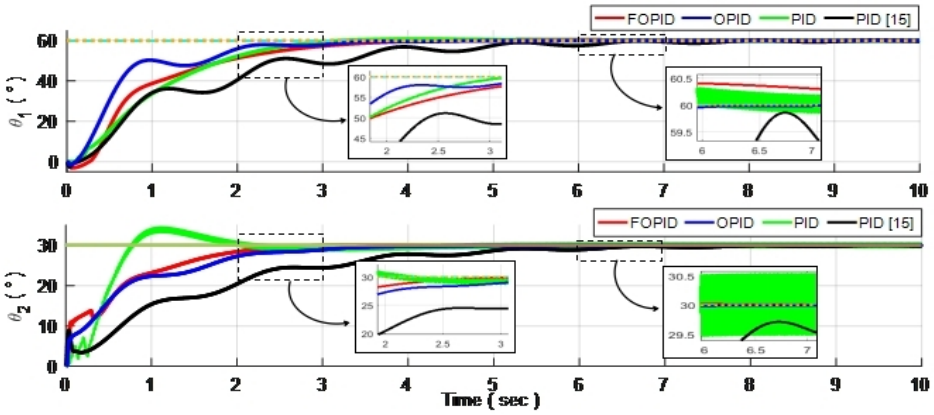

Figure 6. Comparison of the responses obtained for the considered controllers during set-point tracking

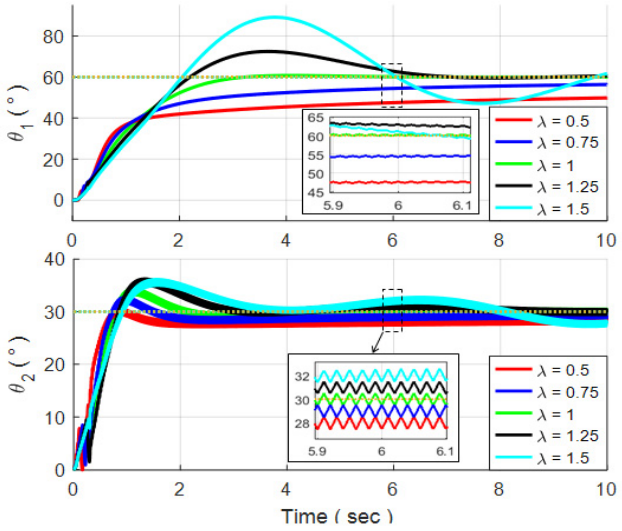

Figure 7. The step responses of μ = 1 and λ with different values

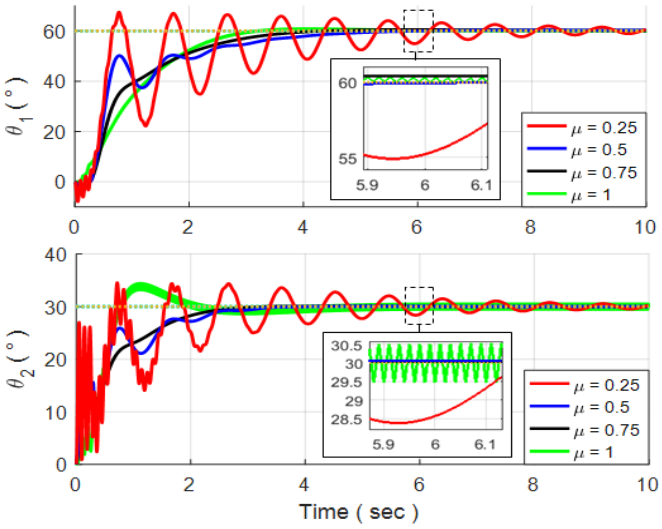

Figure 8. The step responses of $\lambda = 1$ and μ with different values

To inspect the influence of the FOPID's parameters on the control performance in particular the fractional integral order λ and the derivative μ, Figures 7 and 8 compare the property of the step responses of the above set-point tracking when $\mu = 1$, $\lambda = 0.5{:}0.25{:}1$, and $\lambda = 1$, $\mu = 0.5{:}0.25{:}1$, respectively.

4.2 Point-to-point trajectory tracking

This simulation uses the same circular-shaped trajectory of [13] to evaluate the proposed FOPID controller against trajectory tracking. By using the same initial conditions mentioned above, the desired and generated bending angles for both sections and the Euclidean errors between them are shown in Figure 9. From this Figure, it can be seen that the curves are almost super–posed where the average errors are respectively smaller than 0.002° and 0.006°.

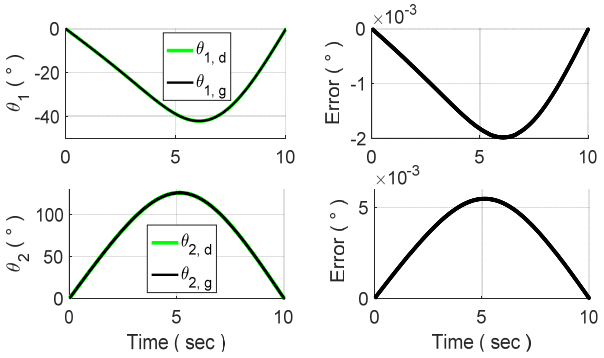

Figure 9. Desired and generated bending angles and Eucli–dean errors between them

To clarify more about the tracking performance of the proposed controller, Figure 10 highlights the desired and generated circular-shaped trajectory and Euclidean errors between them along x - axis and z - axis. This Figure shows that the curves are almost superposed and that the average errors are smaller than 0.002 mm and 0.008 mm along x - axis and z - axis, respectively. These results indicate the good control performance of the proposed FOPID controller. It should be noted that the displayed trajectories in Figure 10 are performed using the kinematics models presented in Equation 1. The required control signals to track the circular-shaped trajectory are shown in Figure 11. From this Figure, it is clear that the proposed controller gives better control performance regarding the smoothness of control signals.

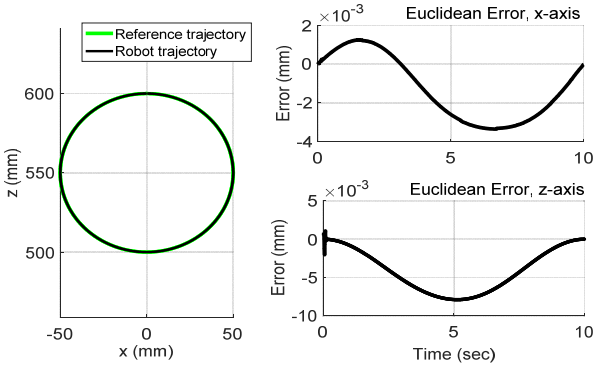

Figure 10. Desired and generated Cartesian trajectories and Euclidean errors between them

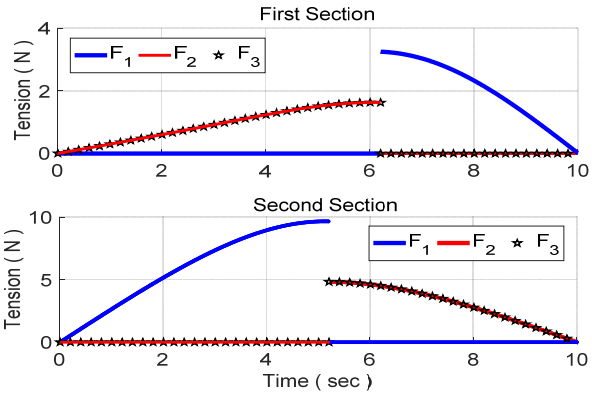

Figure 11. Required control signals to track the circular-shaped trajectory

5. DISCUSSION

The simulation results and a comparison analysis bet–ween the classical PID controllers, OPID controller, and FOPID controller showed that the FOPID is a perfect trajectory tracking dynamic controller because of its flexibility and capability stemming from the fractional order of the integral and the derivative. The control signals of the proposed FOPID controller are smoother

Table 4. Recent contributions in control of CDCRs

Robot	Control techniques	Trajectory accuracy
CDCR: Continuous shape, rigid structure, multi-section, controlled by cables.	Proposed FOPID controller	Accuracy: $< 8 \cdot 10^{-3}$ mm Validation: Simulation of a planar CDCR with two sections using dynamic model
	NMPC-PSO scheme [13]	Accuracy: $< 3 \cdot 10^{-4}$ mm Validation: Simulation of a planar CDCR with two sections using kinematic and dynamic models
	NMPC-PSO scheme [23]	Accuracy: $< 7 \cdot 10^{-4}$ mm Validation: Simulation of a spatial CDCR with two sections using kinematic model
	Optimized Nonlinear Sliding Mode Control [24]	Accuracy: $< 1.38 \cdot 10^{-1}$ mm equivalent to: MSE = $2.3069 \cdot 10^{-5}$ Validation: Simulation of a planar CDCR with two sections using dynamic model.
	PID controller [17]	Accuracy: $< 5.5 \cdot 10^{-1}$ mm Validation: Simulation of a planar CDCR with two sections using dynamic model

and less in amplitude than other controllers. Also, the proposed controller can control the CDCR's end-tip with positioning errors of less than 0.008 mm, representing 0.13% of the total length of the CDCR. Overall, the proposed FOPID controller shows good performance in tracking the accuracy and smoothness of control signals compared to the classical and optimized PID controllers suggested for comparison in this paper.

For comparison, Table 4 lists recent contributions to the control of Cable-Driven Continuum Robots (CDCRs). By analyzing these contributions, it is noted that the best performances are achieved by the FOPID controller except that of Nonlinear Model Predictive controllers based Particle swarm Optimization (NMPC-PSO) [13, 23]. However, considering the simplicity, computation time, and cost, the proposed FOPID controller is better than NMPC-PSO despite the relative lack of precision. As a general conclusion of our analysis, the proposed FOPID controller can be used fruitfully to test essentially other models for all continuum robots.

6. CONCLUSION

This paper proposes a Fractional-Order Proportional-Integral-Derivative (FOPID) controller for the trajectory tracking problem of a class of continuum robots, namely Cable-Driven Continuum Robots (CDCR). The efficacy of the FOPID controller has been demonstrated in set-point tracking and point-to-point trajectory tracking problems and compared to classical and optimized PID controllers and the available literature works. The re–sults confirm that the FOPID controller shows signi–ficant promise as an alternative controller. However, FOPID's parameter tuning is challenging; thus, the PSO algorithm is used for optimal parameters thanks to its simplicity.

As a perspective for this work, we intend to imple–ment the proposed FOPID controller in a 3D dynamic space using an exact model rather than an approximate one as well as taking into account obstacle avoidance during trajectory tracking.

REFERENCES

[1] Kolachalama, S. Lakshmanan, S.: Continuum robots for manipulation applications: a survey, Journal of Robotics, Article ID 4187048, 19 pages, 2020.

[2] Zhang, Y. and Lu, M.: A review of recent advancements in soft and flexible robots for medical applications, The International Journal of Medical Robotics and Computer Assisted Surgery, Vol. 16, No. 3, p.e2096, 2020.

[3] Chen, F. and Wang, M.Y.: Design optimization of soft robots: A review of the state of the art, IEEE Robotics & Automation Magazine, Vol. 27, No. 4, pp.27–43, 2020.

[4] Polygerinos, P., Correll, N., Morin, S.A., Mosadegh, B., Onal, C.D., Petersen, K., Cianchetti, M., Tolley, M.T. and Shepherd, R.F.: Soft robotics: Review of fluid-driven intrinsically soft devices; manufacturing, sensing, control, and applications in human-robot interaction, Advanced Engineering Materials, Vol. 19, No. 12, p.1700016, 2017.

[5] Rao, P., Peyron, Q., Lilge, S. and Burgner-Kahrs, J.: How to model tendon-driven continuum robots and benchmark modelling performance, Frontiers in Robotics and AI, Vol. 7, p.630245, 2021.

[6] Tan, N., Yu, P., Zhang, X. and Wang, T.: Model-free motion control of continuum robots based on a zeroing neurodynamic approach, Neural Networks, Vol. 133, pp.21–31, 2021.

[7] Li, S. and Hao, G.: Current trends and prospects in compliant continuum robots: A survey, in: Actuators, Vol. 10, No. 7, pp. 145, 2021.

[8] Stevanovic, I. and Rašuo, B.: Development of a miniature robot based on experience inspired by nature, FME Transactions, Vol. 45, No. 1, pp. 189-197, 2017.

[9] Lazarević, M.: Optimal Control of Redundant Robots in Human-Like Fashion, FME Transactions, Vol. 33, No. 2, pp. 53-64, 2005.

[10] Barrientos-Diez, J., Dong, X., Axinte, D. and Kell, J.: Real-time kinematics of continuum robots: modelling and validation, Robotics and Computer Integrated Manufacturing, Vol. 67, p.102019, 2021.

[11] Huang, X., Zou, J. and Gu, G.: Kinematic modeling and control of variable curvature soft continuum robots, IEEE/ASME Transactions on Mechatronics, Vol. 26, No. 6, pp.3175–3185, 2021.

[12] Wang, H., Yang, B., Liu, Y., Chen, W., Liang, X. and Pfeifer, R.: Visual servoing of soft robot manipulator in constrained environments with an adaptive controller, IEEE/ASME Transactions on Mechatronics, Vol. 22, No. 1, pp.41–50, 2016.

[13] Amouri, A., Cherfia, A., Merabti, H. and Laib, D.L.Y.: Nonlinear model predictive control of a class of continuum robots using kinematic and dynamic models, FME Transactions, Vol. 50, No. 2, pp. 339–350, 2022.

[14] Webster III, R.J. and Jones, B.A.: Design and kinematic modeling of constant curvature continuum robots: A review, The International Journal of Robotics Research, Vol. 29, No. 13, pp. 1661–1683, 2010.

[15] Qi, F., Chen, B., Gao, S. and She, S.: Dynamic model and control for a cable-driven continuum manipulator used for minimally invasive surgery, The International Journal of Medical Robotics and Computer Assisted Surgery, Vol. 17, No. 3, p.e2234, 2021.

[16] Liu, Z., Zhang, X., Cai, Z., Peng, H. and Wu, Z.: Real-time dynamics of cable-driven continuum robots considering the cable constraint and friction effect, IEEE Robotics and Automation Letters, Vol. 6, No. 4, pp.6235–6242, 2021.

[17] Amouri, A., Zaatri, A. and Mahfoudi, C.: Dynamic modeling of a class of continuum manipulators in fixed orientation, Journal of Intelligent & Robotic Systems, Vol. 91, No. 3, pp.413–424, 2018.

[18] Bousbia, L., Amouri, A. and Cherfia, A.: Dynamics modeling of a 2-DoFs cable-driven continuum robot, World Journal of Engineering, 2022.

[19] Ehsani-Seresht, A. and Hashemi-Pour Moosavi, S.: Dynamic modeling of the cable-driven continuum robots in hybrid position-force actuation mode, Journal of Mechanisms and Robotics, Vol. 12, No. 5, p.051002, 2020.

[20] Zhou, Z., Zheng, X., Chen, Z., Wang, X., Liang, B. and Wang, Q.: Dynamics modeling and analysis of cable-driven segmented manipulator considering friction effects, Mechanism and Machine Theory, Vol. 169, p.104633, 2022.

[21] Xu, W., Liu, T. and Li, Y.: Kinematics, dynamics, and control of a cable-driven hyper-redundant manipulator, IEEE/ASME Transactions on Mechatronics, Vol. 23, No. 4, pp.1693–1704, 2018.

[22] Peng, J., Xu, W., Yang, T., Hu, Z. and Liang, B.: Dynamic modeling and trajectory tracking control method of segmented linkage cable-driven hyper-redundant robot, Nonlinear Dynamics, Vol. 101, No. 1, pp.233–253, 2020.

[23] Amouri, A., Merabti, H., Cherfia, A. and Laib, D.L.Y.: Nonlinear model predictive control for trajectory tracking of a class of continuum robots, UPB Scientific Bulletin, Series D: Mechanical Engineering, Vol. 84, No. 3, pp. 19–32, 2022.

[24] Ghoul, A., Kara, K., Benrabah, M. and Hadjili, M.L.: Optimized nonlinear sliding mode control of a continuum robot manipulator, Journal of Control, Automation and Electrical Systems, pp.1–9, 2022.

[25] Abe, A.: Nonlinear control technique of a pendulum via cable length manipulation: Application of particle swarm optimization to controller design, FME Trans., Vol. 41, No. 4, pp. 265–270, 2013.

[26] Norsahperi N.M.H., Ahmad S., Toha S.F. and Abd Mutalib M.A.: Design, simulation and experiment of PSO-FOPID controller for height position control of a scissor mechanism platform, FME Transactions, Vol. 50, No. 1, pp. 46-54, 2022.

[27] Abed, A.M., Rashid, Z.N., Abedi, F. et al.: Trajectory tracking of differential drive mobile robots using fractional-order proportional-integral-derivative controller design tuned by an enhanced fruit fly optimization, Measurement and Control, Vol. 55, No. 3-4, pp. 209-226, 2022

[28] Ibraheem, G.A.R., Azar, A.T., Ibraheem, I.K. and Humaidi, A.J.: A novel design of a neural network-based fractional PID controller for mobile robots using hybridized fruit fly and particle swarm optimization, complexity, 2020.

[29] Kumar, A. and Kumar, V.: Hybridized ABC-GA optimized fractional order fuzzy pre-compensated FOPID control design for 2-DOF robot manipulator, AEU-International Journal of Electronics and Communications, Vol. 79, pp.219–233, 2017.

[30] Faraj, M.A. and Abbood, A.M.: Fractional order PID controller tuned by bat algorithm for robot trajectory control, Indonesian Journal of Electrical Engineering and Computer Science, Vol. 21, No. 1, pp.74–83, 2021.

[31] Al-Mayyahi, A., Aldair, A.A. and Chatwin, C.: Control of a 3-RRR planar parallel robot using fractional order PID controller, International Journal of Automation and Computing, Vol. 17, No. 6, pp.822–836, 2020.

[32] Xue, D.: Fractional-order control systems: fundamentals and numerical implementations, De Gruyter, Berlin, Boston, 2017.

[33] Podlubny, I.: Fractional-order systems and $PI^{\lambda}D^{\mu}$ controllers, IEEE Transactions on Automatic Control, Vol. 44, No. 1, pp. 208–214, 1999.

[34] Shah, P. and Agashe, S.: Review of fractional PID controller, Mechatronics, Vol. 38, pp.29–41, 2016.

[35] Monje, C.A., Chen, Y., Vinagre, B.M., Xue, D. and Feliu-Batlle, V.: Fractional-order systems and controls: fundamentals and applications, Springer Science & Business Media, 2010.

[36] Zhang, G., Pan, L., Neri, F., Gong, M., Leporati, A.: Metaheuristic optimization: Algorithmic design and applications, Journal of Optimization, 2017.

[37] Parouha, R.P. and Verma, P.: State-of-the-art reviews of meta-heuristic algorithms with their novel proposal for unconstrained optimization and applications, Archives of Computational Methods

in Engineering, Vol. 28, No. 5, pp.4049–4115, 2021.

[38] Svorcan, J., Trivković, Z., Ivanov, T., et al.: Multi-objective constrained optimizations of VAWT composite blades based on FEM and PSO, FME Transactions, Vol. 47, No. 4, pp. 887-893, 2019.

[39] Jerman, B., Hladnik, J., Resman, R., Landschützer, C.: Optimization of the support structure of large axial-radial bearing of overhead type manipulator, FME Transactions, Vol. 46, No. 3, pp. 386-391, 2018.

[40] Kennedy, J. and Eberhart, R.: Particle swarm optimization, in: *Proceedings of IEEE ICNN'95-international conference on neural networks*, Vol. 4, pp. 1942–1948, 1995.

[41] Merrad, A., Amouri, A., Cherfia, A. and Djeffal, S.: A Reliable Algorithm for Obtaining All-Inclusive Inverse Kinematics' Solutions and Redundancy Resolution of Continuum Robots, Arabian Journal for Science and Engineering, pp.1–16, 2022.

[42] Rehman, R., Khan, S.A. and Alhems L.M.: The effect of acceleration coefficients in particle swarm optimization algorithm with application to wind farm layout design, FME Transactions, Vol. 48, No. 4, pp. 922-930, 2020.

[43] Amouri, A., Mahfoudi, C. and Zaatri A.: Contribution to inverse kinematic modeling of a planar continuum robot using a particle swarm optimization, in: *Proceedings of the Multiphysics Modelling and Simulation for Systems Design Conference*, *MMSSD 2014, 17-19 December, Sousse, Tunisia*, 2014.

[44] Noel, M.M.: A new gradient-based particle swarm optimization algorithm for accurate computation of global minimum, Applied Soft Computing, Vol. 12, No. 1, pp.353–359, 2012.

NOMENCLATURE

C	Cosine function.
C_f	Cost function.
D	Generalized operator of integration and differentiation.
e	Trajectory error
f, h	Nonlinear functions.
k	section index, with $k = 1, 2$.
K_{P}	Proportional coefficient
K_{D}	Derivative coefficient
K_{I}	Integral coefficient
ℓ	Section length
lcl	Local, means with respect to local frame
n, b, t	Unit vector of rotation matrix
P	Vector position
R	Rotation matrix
s	State variables
S	Sine function
t	Time
u	Control signal
x, y, z	Cartesian coordinates

Greek symbols

λ	Integrator order
μ	Differentiator order
θ	Bending angle
φ	Orientation angle
ω	Angular velocity

Abbreviations and Acronyms

CCKA	Constant Curvature Kinematic Approach
CDCR	Cable-Driven Continuum Robot
FOPID	Fractional-Order Proportional-Integral-Derivative
MAE	Mean Absolute Error
MSE	Mean Squared Error
NMPC	Nonlinear Model Predictive Control
OPID	Optimized Proportional-Integral-Derivative
P	Proportional
PD	Proportional-Derivative
PI	Proportional-Integral
PID	Proportional-Integral-Derivative
PSO	Particle Swarm Optimization

ДИЗАЈН ПИД КОНТРОЛЕРА ФРАКЦИОНОГ РЕДА ЗА КОНТРОЛУ ПРАЋЕЊА ПУТАЊЕ КОНТИНУАЛНИХ РОБОТА

А. Белхири, А. Амоури, А. Шерфиа

Континуум роботи су продужетак понашања хипер-редундантних робота који су обично инспирисани живим биолошким органима. Ови роботи надмашују своје круте колеге у погледу високе флекси–билности, спретности и што је најважније безбедне интеракције. Са друге стране, они су кинематички редундантни, веома нелинеарни и са више улаза, и сходно томе, њихово управљање остаје сложен и изазован задатак. У ту сврху, овај рад предлаже контролер разломачног реда пропорционално-интегрално-деривативни (ФОПИД) за контролу крајњег врха робота континуума.

Предложени контролер је дизајниран да контролише улазе класе континуалних робота, односно Кабловски континуални робот (CDCR). Да би се контролер дизајнирао на задовољавајући начин, алгоритам Оптимизације роjем честица (PSO) издваја оптималне вредности параметара контро–лера.

Ефикасност и перформансе контроле предложеног ФОПИД контролера демонс–тирани су кроз два примера симулације: праћење задате тачке и праћење путање од тачке до тачке. Поред тога, добијени резултати симулације се пореде са онима које дају класични и оптимизовани ПИД регулатори

и са неким доступним шемама. Имајући у виду добијене резултате, јасно је да су перформансе предложеног ФОПИД контролера супериорне у тачности праћења и глаткости контролних сигнала.